# ON 3D TRACKING FOR ECHOCARDIOGRAPHIC CLASSIFICATION OF ACUTE MYOCARDIAL INFARCTION

**Eyal Braiman and Moshe Porat**

Department of Electrical Engineering
Technion - Israel Institute of Technology
Haifa, Israel 32000
Email: braiman@tx.technion.ac.il, mp@ee.technion.ac.il

## ABSTRACT

*Accurate characterization of acute myocardial infarction (AMI) is crucial for the management of the patient. In this work we present a method for 3-dimensional (3D) velocity estimation and object tracking in sequences of ultrasound volume scans. Velocity estimation is based on motion estimation in 3D with maximum likelihood criteria. Tracking is carried out using a data association method based on location and velocity. The proposed algorithm has been tested on various data sources and on in-vivo 3D volume scan of the left ventricle, providing very useful results for the characterization of AMIs.*

## 1. INTRODUCTION

For patients presenting with a chest pain, rapid diagnosis of Acute Myocardial Infarction (AMI) is important for further management and possible salvage of the myocardial tissue. Ultrasound is an important adjunct to the well-accepted diagnostic tools such as ECG and serum enzymes, especially when the other predominant signs are missing or ambiguous. Wall motion abnormality is the earliest symptom of a nearing AMI, however, specific pattern analysis is needed to classify the situation correctly.

Ultrasound scans of the heart, including 3D scans at high frame rates, are widely available today and used to diagnose various heart diseases. Detecting abnormalities in the wall motion function has become of major importance since reduced motion has correlation with an ischemic muscle action. Automatic movement tracking of the heart walls and calculating their local velocities can make the diagnoses more accurate and useful.

Estimating local velocities in ultrasound scans presents several challenges [6]. The major difficulty is that ultrasound images have high Rayleigh governed speckle noise and Gaussian distributed electronic noise, resulting in a low signal to noise ratio (SNR). In addition, the tissue pattern is varying fast and its motion includes deformation in addition to rotation and translation. The resolution of the images depends on the ultrasound equipment and it usually has high axial resolution and low angular resolution. Working with 3D scans instead of 2D images naturally adds another complication due to an additional motion dimension; however, it eliminates the problem of 'out of plane motion' found in 2D scans.

## 2. THE PROPOSED ALGORITHM

We start with the description of the algorithm.

### 2.1. Data Acquisition

In this work we use 3D data and B-mode scans of the left ventricle to test the proposed algorithm. The algorithm is applied directly to the 3D data without any modifications or transformations.

### 2.2. Maximum likelihood Criteria

We represent two consecutive scanned volumes by *X* and *Y*. Let $I(x_i)$ be the intensity of a macro block at coordinates $x_i = \{x_{ijk}\} \in X$ and $I(y_i)$ be the intensity of a macro block at coordinates $y_i = \{y_{ijk}\} \in Y$, where *i* represents all possible macro blocks and *j,k* are coordinates within the macro block. Let $v_i = \{x_i - y_i\}$ be the displacement vector between the two macro blocks $x_i$ and $y_i$. Based on the above notations, the maximum likelihood (ML) estimation based on [2], [1]is:

$$v_i^{ML} = \arg\max_{v_i} \left( I(x_i) \mid I(y_i), v_i \right). \qquad (1)$$

There are several models describing ultrasound images with either multiplicative or additive noise. A common model that was used in this work assumes multiplicative Rayleigh distributed noise with distribution function given in [3]:

$$f_x(x) = \frac{x}{\sigma^2} \exp\left( -\frac{x^2}{2\sigma^2} \right). \quad x > 0 \qquad (2)$$

We denote the noiseless value of pixels in macro block *i* by $s_{ijk}$. Assuming statistically independent noise, the model for pixels in the macro blocks is:

$$\begin{aligned} x_{ijk} &= \eta_{ijk}^x s_{ijk} \\ y_{ijk} &= \eta_{ijk}^y s_{ijk} \end{aligned}, \qquad (3)$$

where $\eta_{ijk}^x$ and $\eta_{ijk}^y$ are two independent noise elements with Rayleigh distribution. Using (3), we obtain:

$$x_{ijk} = \eta_{ijk} y_{ijk}, \quad \eta_{ijk} = \frac{\eta_{ijk}^x}{\eta_{ijk}^y}. \qquad (4)$$

$\eta_{ijk}$ is a division of two independent noise elements with Rayleigh distribution given in (2), having the following distribution [4]:

$$f_\eta(\eta) = \frac{2\eta}{\left(\eta^2+1\right)^2}, \quad \eta > 0 \ . \tag{5}$$

The probability function for this distribution is [2]:

$$\mathrm{p}\left(\mathrm{x}_\mathrm{i} \mid y_i, v_i\right) = \prod_j \prod_k \left[ \frac{f_\eta\left(\frac{x_{ijk}}{y_{ijk}}\right)}{y_{ijk}} \right] = \tag{6}$$

$$= \prod_j \prod_k \left\{ \frac{2x_{ijk}}{y_{ijk}^2 \left[ \left(\frac{x_{ijk}}{y_{ijk}}\right)^2 + 1 \right]^2} \right\},$$

and its maximization is equivalent to maximization of (1). Taking the natural logarithm of both sides of (4), we obtain the following model:

$$\tilde{x}_{ijk} = \tilde{y}_{ijk} + \tilde{\eta}_{ijk} \ \ where \ \tilde{x}_{ijk} = \ln\left(x_{ijk}\right), \tag{7}$$
$$\tilde{y}_{ijk} = \ln\left(y_{ijk}\right), \tilde{\eta}_{ijk} = \ln\left(\eta_{ijk}\right).$$

Accordingly, the probability function as in (6) is given by [4]:

$$\mathrm{p}\left(\mathrm{x}_\mathrm{i} \mid y_i, v_i\right) = \prod_j \prod_k \left[ \frac{x_{ijk} f_\eta\left(\frac{x_{ijk}}{y_{ijk}}\right)}{y_{ijk}} \right] = \tag{8}$$

$$= \prod_j \prod_k \left\{ \frac{2\left(\frac{x_{ijk}}{y_{ijk}}\right)^2}{\left[ \left(\frac{x_{ijk}}{y_{ijk}}\right)^2 + 1 \right]^2} \right\}.$$

This probability function is used in this work in Motion Estimation algorithm, as described in following sub-section.

### 2.3. Motion Estimation (ME)

The motivation for using ME is to trace movement of objects from one ultrasound frame to the next. It is assumed that the objects undergo small changes (or none) from frame to frame due to high frame rate. Therefore each frame is divided into matrix of non-overlapping macro blocks such that:

$$X = \bigcup_i x_i \quad x_i \bigcap x_j = \varnothing \ for \ i \neq j$$
$$Y = \bigcup_i y_i \quad y_i \bigcap y_j = \varnothing \ for \ i \neq j \ . \tag{9}$$

Each block in the current frame $X$ is compared with the corresponding block at the same coordinates and its neighbors in the following frame $Y$ (search window 3D) as shown in Fig. 1.

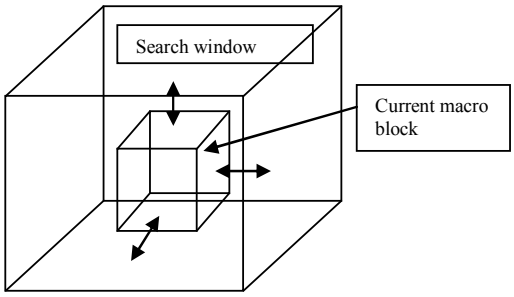


Figure 1 – Matching a macro block from a current frame to a macro block inside the search window in the following frame

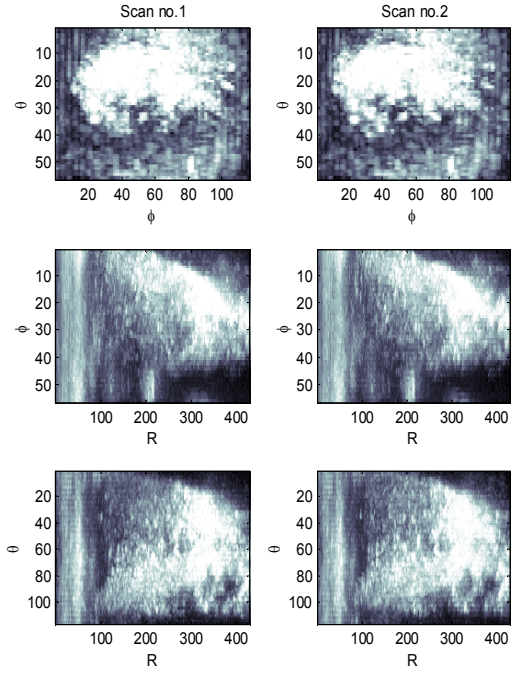


Figure 2 – Two consecutive in-vivo scans: (a) scan no.1; (b) scan no.2. Each image presents two of the three dimensions: R represents the range bins, θ is the out the plane angle and φ is the on the plane angle measured in degrees

In this work we use an *Exhaustive Search* (ES) algorithm for finding the best match [5]. This algorithm is also known as *Full Search* and searches in all possible locations within the 3D search window. Although this algorithm is somewhat complex; it provides the most accurate results since all the possibilities are examined. The cost function used to define the best match is the maximum likelihood criterion defined in (8). A macro block in the search window that has the highest maximum likelihood value is chosen as the location to which the current macro

block has moved (i.e., best match). The output of ME function is the displacement in terms of pixels of each macro block of the current frame in each of the three dimensions.

The ME is calculated only for macro blocks that are above the mean noise level. This level is calculated here as an average value of 1000 samples taken randomly from the scanned volume. We based this value on an assumption that the scanned tissue occupies only a small part of the volume and the rest of it is noise, as can be seen for example in Fig. 2. By doing so we reduced the number of calculations as well as the number of false tracks caused by apparent movements of macro blocks that do not include tissue information.

This way the best match is calculated for all the blocks in every frame. The displacement vectors are used to build tracks of the tissue movement as described in the next paragraph.

### 2.4. Tracking

Estimation of temporal velocity vectors of different macro blocks is not sufficient when the purpose is detecting abnormalities in tissue movement. If we wish to diagnose tissue condition, we have to examine the velocities for a prolonged period of time. We propose to follow the tissue movement from frame to frame, or literally track its behavior.

To achieve this goal, the tracks were created by connecting sequential displacement of each macro block and thus allowing the algorithm to examine tissue movement through all the scans.

No smoothing or prediction were applied, and data association, i.e., deciding which macro block belongs to which track, is based on the block matching technique described in 2.2.

Let $x_i^1$ be a macro block in the first frame. Using ME with maximum likelihood criteria we find the macro block in the following frame, which is the best match for $x_i^1$ and denote it $x_i^2$. We repeat the process for $x_i^2$ and the following frames to get a vector $x_i^n = \{x_i^1, x_i^2, x_i^3, \ldots\}$, where $n$ represents the frame number, containing displacements of the initial macro block $x_i^1$ through $n$ frames. We repeat the process for all the macro blocks in the initial frame.

## 3. RESULTS

The proposed algorithm has been tested first with simulated data and then with real in-vivo 3D images, as described in the following sub-sections. The simulated data was instrumental in comparing the algorithm's results to the characteristics behind the model by which the simulated data was generated.

### 3.1. Simulation

In order to examine the performance of the ME algorithm with ML, simulated data was generated. We constructed 3D images with low valued background and high valued cubic shaped object. These images were multiplied by a Rayleigh distributed noise term. The original image with and without noise is shown in Fig 3.

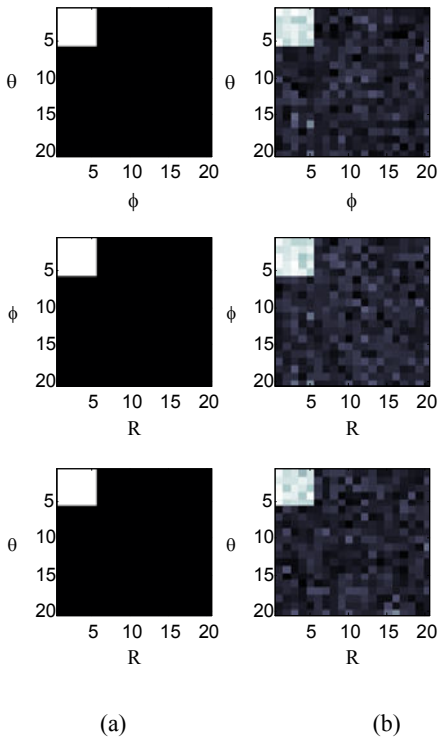


Figure 3 – The simulated data. Each image presents two of the three dimensions: (a) original data; (b) data with Raleigh distributed noise

The 3D data is projected onto two of the three dimensions by taking only the maximum intensity for one of the axes (range, out the plane angle or on the plane angle). We chose this method of presentation due to the difficulties in presenting volumetric data in 2D. Shifted versions of the original image were created and multiplied by an independent Rayleigh distributed noise term. We applied the proposed algorithm to the simulated data containing a rectangular object moving in two of the three dimensions (range and the on the plane angle) and the results for three consecutive scans are shown in Fig. 4. The calculated movements in every plane are represented by an arrow. As can be seen in Fig. 4, the algorithm accurately tracks the movement of the object and there are no false motions detected due to the background noise since the ME was calculated only for macro blocks that are above the noise level, as described in 2.3.

### 3.2. Left ventricle scans

Having verified that our algorithm works correctly on simulated data, we tested it on in-vivo data. In our tests, 8 sequential scans of the same volume were used to calculate tissue displacement and to track the movements of the macro blocks during the scans. The scans were divided into macro blocks of 5×5×5 pixels. The tracks that contain movement for all 8 scans and their initial macro block

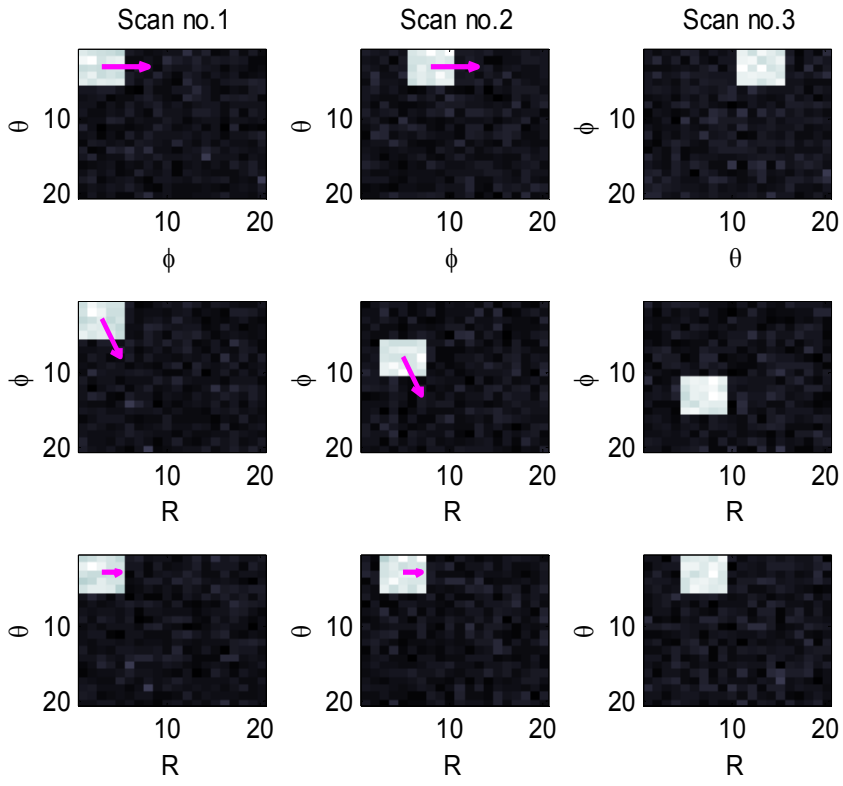


(a) (b) (c)

Figure 4 – Three consecutive scans of the simulated data with displacement vectors. Each image presents two of the three dimensions: (a) scan no.1; (b) scan no.2; (c) scan no.3

have passed the noise threshold, as described in 2.3, are shown in Fig 5. The calculated movements from frame to frame are represented by a single arrow. Connected arrows represent single tracks.

Tissue displacements vectors of the first two consecutive scans are presented in Fig 6. The 3D scans are projected on two of the three dimensions by taking only the maximum intensity for one of the axes, as was done in Fig. 2 and for the simulated data. Motion vectors in two of the three dimensions are plotted over the data.

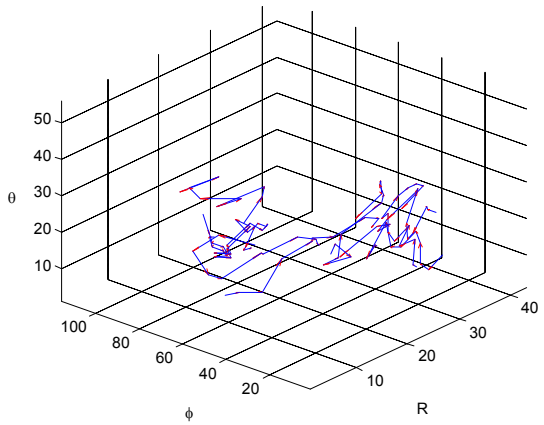


(a)

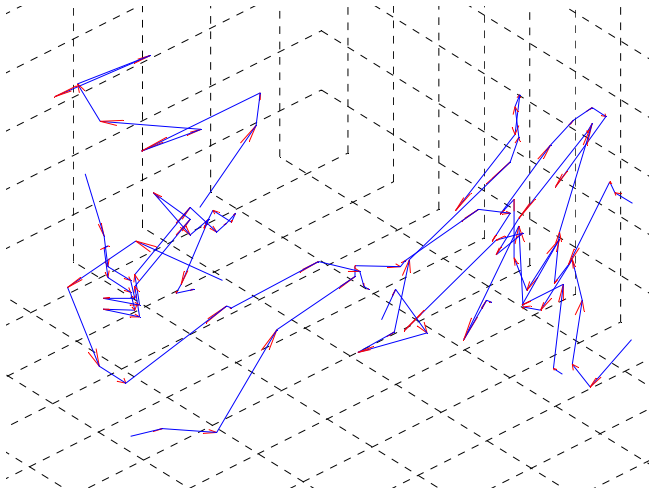

(b)

Figure 5 – (a) Tracks built based on consecutive displacements using in-vivo data. R represents the range bins, θ is the out the plane angle and φ is the on the plane angle measured in degrees; (b) zoom-in at the tracks. Due to complex motion of the tissue some tacks overlap and zigzag, but other tracks are easy to follow.

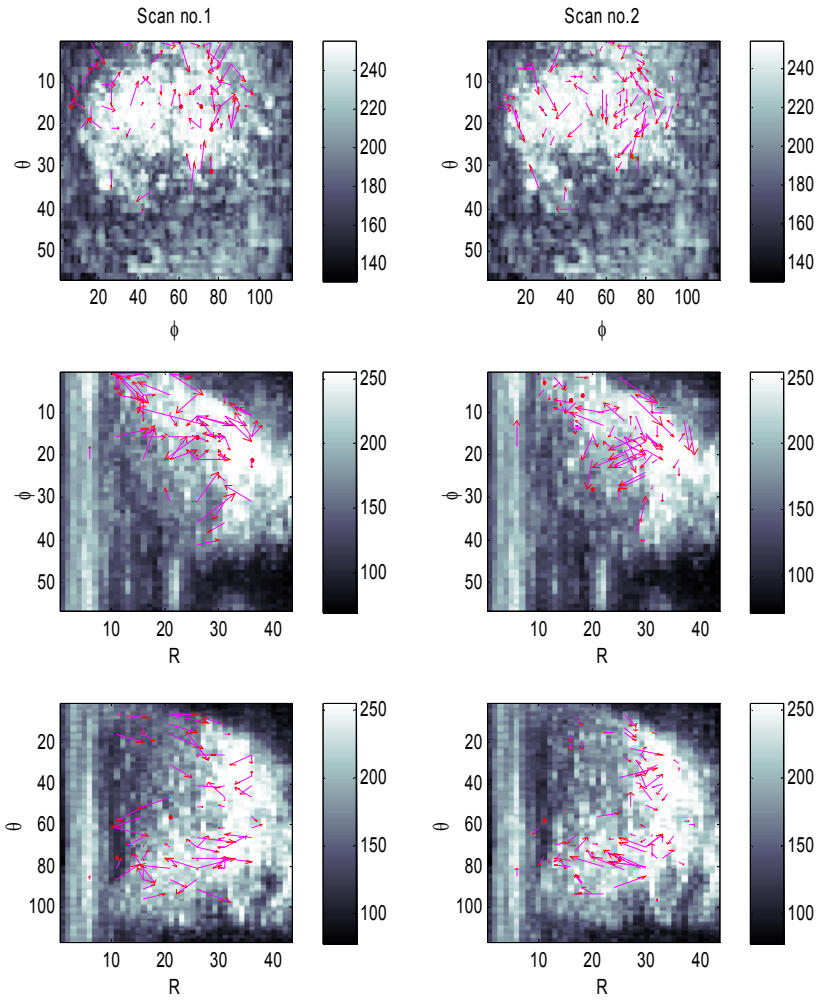


(a) (b)

Figure 6 – Two consecutive in-vivo scans with displacement vectors. Each image presents two of the three dimensions: (a) Scan no.1; (b) Scan no.2

## 4. CONCLUSIONS

Long term tracking and velocity estimation using ME with maximum likelihood criteria has been proposed. Our test results using real in-vivo data show that this method can be used for ultrasound 3D scans in order to analyze tissue behavior for prolonged period. This approach is suitable for practical use in ultrasound scan of many types of tissues, including the myocardium, as in this case. The complexity of the proposed algorithm is low and can be easily performed in real time, making it instrumental in the classification of AMIs.

**ACKNOWLEDGEMENT** This work was supported in part by the German-Israeli Foundation (GIF), by the H. & R. Sohnis Cardiology Research Fund, and by the Ollendorff Minerva Centre. Minerva is funded through the BMBF.

## REFERENCES

[1] D. Boukerroui, J.A. Nobble, M. Brady, "Velocity Estimation in Ultrasound Images: a Block Matching Approach", Information processing in Medical imaging (IMPI), 2003. pp. 586-598.

[2] B. Cohen and I. Dinstein: "New maximum likelihood motion estimation schemes for noisy ultrasound images", Pattern Recognition 35, 2002, pp. 455–463.

[3] C. Kotropoulos, X. Magnisalis, I. Pitas, M.G. Strinzis, "Nonlinear ultrasonic image processing based on signal-adaptive filters and self organizing neural nets", IEEE Trans. Image Process. 3 (1), 1994, pp. 65–77.

[4] A. Papoulis, "Probability, Random variables and Stochastic Processes", McGraw-Hill, New York, 1991.

[5] D. Salomon, "Data Compression" 3rd ed., Springer-Verlag New York, 2004. Ch. 6.4.

[6] A. Thrush and T. Hartshorne, "Peripheral Vascular Ultrasound", 2nd Ed., Elsevier, 2005 Ch. 2.